Title	Measurement of driver's visual attention capabilities using real-time UFOV method
Author(s)	Danno, Mikio; Kutila, Matti; Kortelainen, Juha M.
Citation	International Journal of Intelligent Transportation Systems Research vol. 9(2011):3, pp. 115-127
Date	2011
URL	http://dx.doi.org/10.1007/s13177-011-0033-1
Rights	Copyright © (2011) Springer. Reprinted from International Journal of Intelligent Transportation Systems Research. This article may be downloaded for personal use only

Measurement of Driver's Visual Attention Capabilities Using Real-time UFOV Method

Mikio DANNO[*1] Matti Kutila[*2] Juha M. Kortelainen[*3]
Toyota InfoTechnology Center Co., Ltd.[*1]
(6-6-20, Akasaka, Minato-ku, Tokyo, Japan 107-0052, +81-3-5561-8234, danno@jp.toyota-itc.com)
VTT Technical Research Centre of Finland[*3]
(P.O. Box 1300, FI-33101 Tampere, Finland, Tel. +358 20 722 3619, matti.kutila@vtt.fi)
VTT Technical Research Centre of Finland[*4]
(P.O. Box 1300, FI-33101 Tampere, Finland, Tel. +358 20 722 3644, juha.m.kortelainen@vtt.fi)

This paper proposes a new real-time method to measure the driver's useful field of view (UFOV) while driving a car in ordinary traffic situations in an urban environment. This is called the real-time useful field of view (rUFOV) method to discriminate it from conventional UFOV measurement, which is typically performed offline and with laboratory equipment developed by Visual Awareness Inc. The proposed real-time method first tracks traffic objects that appear in the driver's peripheral vision using a road video camera, checks the degree of the driver's attention to these objects using a driver monitoring camera, and finally calculates the percentage reduction in the driver's UFOV using a database acquired over an extended period of time. Preliminary results showed better performance than originally expected. The rUFOV method was then incorporated into a driving simulation environment to enable more precise measurement of the driver's gaze angle. This enabled the performance of safer tests for identifying conditions under which mental load reduced the driver's visual capabilities, thus increasing the possibility of hasty driving, as well as the incorporation of more accurate control parameters into simulation software for risky driving scenarios. Consequently, this paper proposes a new methodology for measuring the driver's UFOV as a potential real-time driver support system with automatic intrusive HMI adaptation and immediate alarm functions. The evaluation was conducted in two phases. First, the system was tested in real traffic using typical vehicle equipment and technically worked with a performance level of 81%.In the second phase, more test runs were performed in the simulator environment, which enabled near accident scenarios to be created without risking traffic safety and it was also measured its reaction time..

Keywords: *Driver's attention, Driver support system, Image processing, Optical flow, Peripheral vision, UFOV*

1. Introduction

It has been reported that the reduced visual attention capabilities of elderly drivers may increase the risk of traffic accidents [1]. It has also been reported that a driver's useful field of view (UFOV) not only decreases with age but also at higher driving speeds and under the influence of drugs or mental workloads such as stress [2]. The measurement of visual capabilities such as UFOV is gaining in importance since the relative number of elderly drivers is increasing in industrial countries [3]. The driving capabilities of elderly drivers may be adversely affected by a decline in attention abilities combined with slower reaction times. However, as complex traffic situations become more common, drivers are often required to have better attention abilities than ever before. Owsley et al. reported that older drivers with a UFOV impairment of 40% or higher were 2.2 times more likely to be involved in a crash than other drivers (N=294), showing that UFOV is highly capable of predicting the crash involvement of older drivers [4].

Conventionally, UFOV is measured by offline methods that identify the area from which visual information can be extracted at glance without movement of the head or eyes. However the effectiveness of this method is reduced if the subject has poor vision. It also has limited capability to consider divided attention and the ignoring of distractions, and its processing ability is slow.

Previous studies measured drivers' UFOV using offline methods in a laboratory. Several alternative UFOV measurement methods have been suggested. The first used a large touch screen with a mouse, which was incorporated later into medical examinations [2]. The second established a method that enabled better control of the viewing angle of the peripheral stimulus within a range of 10 to 35 degrees of eccentricity. In these PC-based methods, only the duration of the stimulus time and the eccentricity of the constant peripheral stimulus could be controlled.

In these methods to measure UFOV, subjects are instructed to perceive objects on a PC display. Software is then used to control both the duration of the stimulus

and the eccentricity. The percentage reduction in UFOV is calculated based on the accuracy of responses for varying stimuli eccentricities and durations.

These methods are only capable of examining visual acuity, and it is difficult to use them to define the useful visual field and the speed of processing. As a result, their results may only demonstrate the ability of the driver to perceive frontal objects in complex traffic situations. However, this is a vital element that the driver must be aware of in complex traffic environments like cities. This paper proposes a new real-time method to measure the driver's useful field of view while driving a car under normal traffic situations. This is called the real-time useful field of view (rUFOV) method to differentiate it from standard UFOV measurement, which is usually performed off-line and with laboratory equipment.

The results presented in this paper are intended to indicate that a reduced UFOV is a serious problem when considering driver reaction time. The results show that driver reaction time may increase from 0.2 seconds to a few seconds if the driver's UFOV decreases. Conventionally, UFOV is measured when the driver's capabilities are tested before a driving license can be obtained. However, the intention of this research is to bring the UFOV principle inside the vehicle to assess driver characteristics real-time.

Since the driver's peripheral view may be impaired due to alcohol, fatigue or conversation with another occupant of the vehicle, it would be preferable to measure the driver's UFOV in real-time instead of during an annual check for renewing the driver's license. This system has the potential to significantly improve traffic safety, which is one major policy of governments throughout Europe [5].

The experiments had been conducted in the intersection area, which was the most complex traffic scenario. According to the European Road accident database [15] [16], 43 % of all injury accidents happens in intersection, with an annual total number of accidents of 570,000 in the EU-27 member states. Moreover, 16-36% of all fatal accidents were related to intersection safety. Therefore, we selected an appropriate test scenario as if a vulnerable road user were approaching the intersection area out of the driver's peripheral view.

2. rUFOV Concept

2.1. System

In driving, peripheral vision is used to detect information that may be important to safe driving. This kind of information includes road signs, potential hazards, and changes in traffic flow. After noticing something important, a driver will first normally move their eyes in the direction of the event of interest, followed by the head. The finest spatial detail that can be perceived with central vision is defined by the term "visual acuity". Impaired visual acuity in the central vision may result in the driver failing to read signs or recognize hazards.

A driver's attention capability is dependent on the task, and the UFOV becomes narrower with increasing mental load. Thresholds and response latencies also grow with the eccentricity of stimuli due to the inferior performance of peripheral vision. Therefore, it is necessary to take both the position of an external object and the mental load of the task into account when studying a driver's performance [2] [6].

The rUFOV measurement system includes two video camera systems connected to a PC. The first is a road camera for monitoring the road to measure the capability of driver's peripheral vision (to understand whether a driver is detecting information or not). The second is a driver-monitoring camera that detects the driver's direction of gaze and head movement shown in Fig. 1.

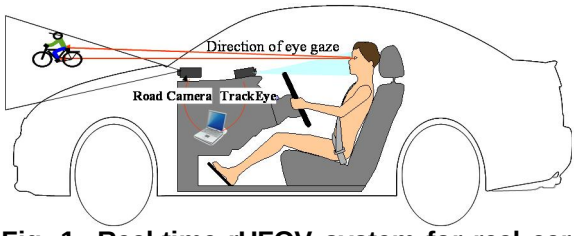

Fig. 1 Real-time rUFOV system for real car driving tests

The proposed rUFOV measurement method is to analyze the drivers' capability of capturing objects in their peripheral vision during normal driving. The appearance of emerging traffic objects in the periphery of the vehicle is compared with the driver's gaze angle. It was assumed that most drivers would normally glance at each emerging object that appeared in their peripheral vision. Therefore, the main focus point for the driver's attention is based on measurement of the driver's gaze angle.

Monitoring a driver's behavior is said to be a complex problem. Even if a fully automatic driver behavior tracking system is adopted, it is not possible to obtain totally reliable results for the degree of driver attention to an emerging peripheral object. Therefore, a statistical database acquired over a long period of time was used. At the same time, a driver may sometimes reduce speed directly without looking at a peripheral object that has been detected. Therefore, both vehicle speed and steering position is used as secondary feedback indices of the status of the driver's attention. The aim of such a basic system is to establish a driver state monitoring function that delivers driver information related to the state of the UFOV.

The flowchart for this system is shown in Fig. 2. A traffic situation measured with the road camera is recorded in a traffic situation data base (DB) on an actual road where the moving object exists according to the moving object detecting function of this system, and

the moving object is detected by the optical flow algorithm.

The confirmation function of this system confirms the normal driving situation from a traffic situation measured with the road camera. The record in the glance DB of driver's gaze direction/vector with the driver monitor camera begins when it is confirmed that the car is running and a moving object is detected.

When the moving object is detected, the moving information calculation function of this system measures the moving regions of the object. The viewing regions calculation function of this system measures the driver's viewing regions based on his gaze direction/vector data and output its data.

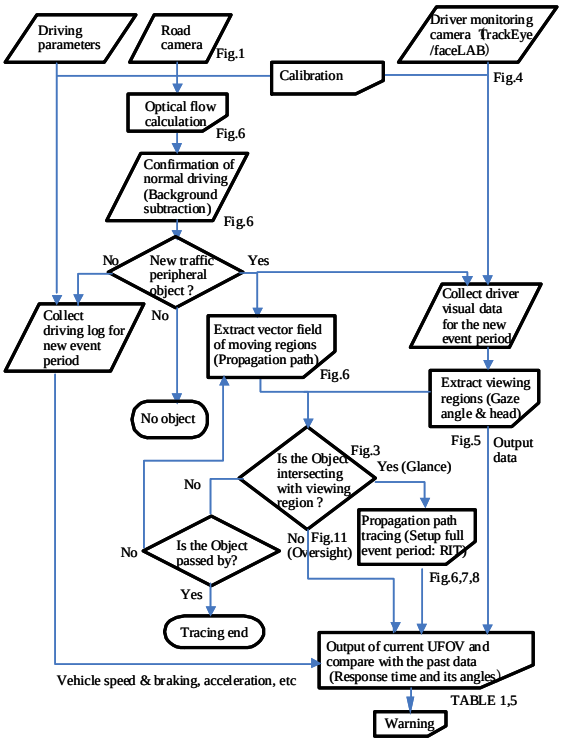

Fig. 2 Flowchart of current UFOV measurement The related figures and tables are indicated in each box.

The intersecting judgment function of this system decides whether the moving regions of the object and the viewing regions of the object are intersecting or not. When it is judged as intersecting, the UFOV calculation function of this system calculates based on the output relating to the measured gaze direction/vector data.

When it is judged as intersecting, based on the results of both the appearance time of the moving object calculation function and the past traffic situation that has been recorded, a driver's UFOV will be calculated.

Based on the above output, this system provides a warning means to give a prescribed warning.

2.2. Detection of objects in the driver's field of view

The macula of the retina normally corresponds to the central 13 degrees of the visual field and the fovea to the central 3 degrees. In the United Kingdom for example, the minimum vision field requirement for driving is 60 degrees either side of the vertical meridian and 20 degrees above and below the horizontal [7].

In Fig. 3, Ca and Cb show the driver's central vision region measured with the driver's monitoring camera and Pr shows the driver's peripheral view regions measured with a road camera. The image frame of a road camera is shown on the top of Fig. 3 and the lowest part shows the overall view from above.

Central vision Ca and Cb are shown with angle β (from β1 the range to β2), peripheral region Pr is shown with angular parameter α (on moving direction the range left side from -α2 to -α1, and on moving direction right side the range from α1 the range to α2). As for the angular parameter α, it measures from the centerline X in the moving direction of the road camera. In the case of the wide angle lens of the road camera 125° according to the minimum vision field requirement for driving [7], angular parameter α2 becomes the 62.5°. The angular parameter α1 shows the limit inside the peripheral region Pr (for example 30° in this case). But, those values may be adjustable according to the driver's central vision C and peripheral vision Pr. The central vision C region of the driver is shown with β2-β1, changes with the visual angle β0 of the driver. β2-β1 is assumed as 26°. The angle β0 is the output result of the driver monitoring system using the driver monitoring camera and it depends on the resolution of the camera system.

Furthermore, the central vision Ca's starting point and starting point of peripheral region Pr have slipped. This reflects the distance of the road camera's location (the right hand side of the vehicle) and the driver monitoring camera's location (the left side).

Fig. 3 shows the situation in which the driver looked at the right side of the bicycle. The driver first has carefully observed the front, but when the bicycle is detected with the peripheral vision Pr, the bicycle is carefully perceived in his central vision Cb. Then, if we measure the time difference between the appearance time of the bicycle in the peripheral vision Pr (at Time A) and the driver perceiving the bicycle in his central vision Cb (at Time B), we can obtain the reaction time from the traffic circumstance DB recorded by the road camera. The intersection detects when the visual angle β0 obtained by the driver monitoring camera enters the range of the angular parameter between α1 and α2 of the road camera. The driver's UFOV is the visual angle β0.

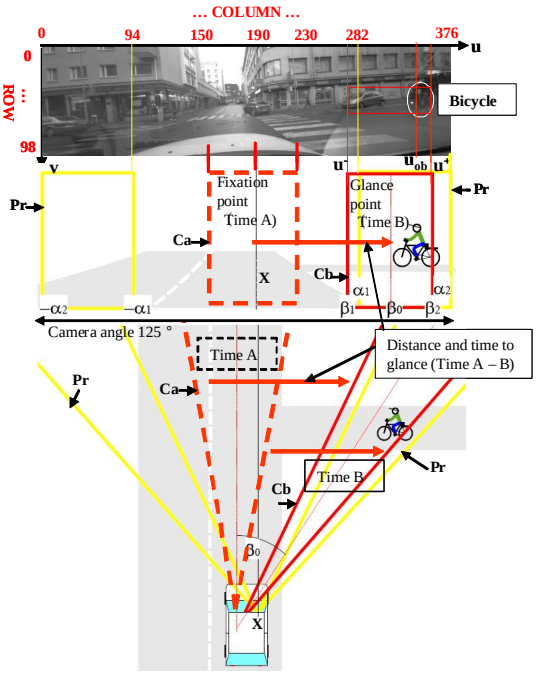

Fig. 3 Measured coordinates

When a bicycle approaches the intersection from the right, the driver turns to look at the bicycle. The upper graph shows that when the driver was gazing forward, he detected a bicycle from the right side (time A). The bottom graph shows that the driver moved his gaze direction to the right in a few seconds and then perceived the bicycle in his central vision field (time B).

In the program, the procedure to measure the driver's viewing angle is to firstly read the driver's viewing angle data of 60 degrees from TrackEye, and then it scales linearly to the image of COLUMN 376 pixels with that angel data. When the peripheral object comes close enough to the front region, such as +-13 degrees (COLUMN 150-230) and moves from the right hand side of the image, the tracing shall be end.

Note that the image width is 0 and 376 pixels in the road camera frame corresponding to the viewing degree of +- 63 degrees, and 94, and 282 column pixels is +- 30 degrees.

It designates the appearance time of the moving object as Ta, and yaw angle of the driver's gaze direction in that detected time (horizontal direction) as Φ a. The time when the driver perceives the moving object is designated as Tb, and yaw angle of his gaze direction is designated as Φ b. The measured coordinate of the central vision range is shown as (u^-, u^+) horizontally and, the coordinate of the moving object's position is (u_{ob}, v_{ob}), the intersection of the driver perceiving the moving object is defined as follows.

$$u^- \le u_{ob} \le u^+ \qquad (1)$$

Furthermore, the time to observe (reaction time): T [sec], the moved angles (yaw angle) Φ [degree] (such as β0), the reaction speed: S [degree/sec] is defined by the following formula (2) from (4) with.

$$T = Tb - Ta \qquad (2)$$

$$\Phi = \Phi b - \Phi a \qquad (3)$$

$$S = \Phi / T \qquad (4)$$

In the filed test, the TrackEye method can achieve a 5 Hz sampling rate to be able to check only if the driver is looking approximately in the direction of the object. Thus, Tb would be triggered by initiation of eye-movement or head-movement in the correct direction or slowing down the car speed. However, in the driving simulator test, the above calculation was made and verified change of UFOV with those indexes.

If any reduction can be found by comparing with past (standardized) values after the difference in the current value of reaction speed value Sc and the past value of Sp, the system will warn the driver.

$$Sc < Sp \qquad (5)$$

3. Field Test

3.1. Experimental equipment

The measurement system for the test car was set up to carry out a preliminary performance analysis. The road camera was placed behind the windscreen on the right-hand side, next to the rear-view mirror. This camera was a uEye UI-1225LE-M model manufactured by IDS Imaging. It used a 1/3-inch MT9V032 monochrome CMOS sensor with wide-VGA resolution (752x480 pixels). A wide-angle lens with a horizontal width of 125° manufactured by Edmunds (NT62-050 objective) was used to allow imaging of the sector of the driver's peripheral vision. Driver monitoring was performed by a low-cost web-camera, connected by USB to a PC as shown in Fig. 4. The driver monitoring camera was located on the instrument panel inside the vehicle, behind the steering wheel and facing the driver.

Fig. 4 Driver-monitoring camera

TrackEye software was selected since it is more practical for use in an actual passenger car. The image processing core was based on the free Open CV computer vision library [8]. Originally, it provided eye

and head locations from either video file or web camera showing the face of a human (Fig. 5). Because the rUFOV concept is based on gaze and head orientations as input calculations have been added to the TrackEye software [9]. The experiments indicated that performance of the low-cost eye tracking system is sufficient for evaluating whether the proposed rUFOV algorithm works, but when implementing real in-vehicle product, a more sophisticated eye tracker is needed.

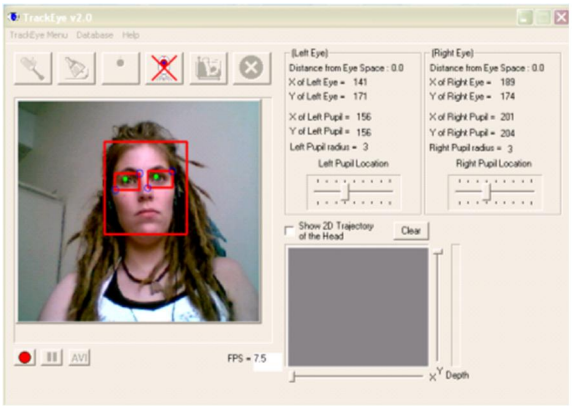

Fig. 5 TrackEye

The software interfaces were adapted for a better fit with the in-vehicle system. The software allowed recording the driver's head and gaze orientations and assessed where the driver was looking at a frame rate of 10 Hz. This calculates the driver's gaze direction with a spatial resolution of 1°. Due to the low-cost USB camera and, most importantly, the driver's eye characteristics concerning the ability to observe peripheral objects, the practical spatial resolution level was about 3-5°. This performance was acceptable for capturing the moment when the driver first observes the object. Turning of the head and eyes was just an indication of detection in the peripheral view. The TrackEye software includes some alternative algorithms for detecting face movement. The Haar face detection algorithm was selected, which seemed to produce better results than the CamShift algorithm. The template matching algorithm was selected for detection of eye movement.

3.2 Driving conditions

The aim of the rUFOV measurement method is to analyze the driver's peripheral vision under normal driving conditions. A sharp turn in driving direction causes difficulties for the optical flow algorithm as the background scenery also shifts significantly in a horizontal direction. Strong acceleration or breaking may cause the vehicle to lift briefly upwards or downwards, thus affecting the background and causing it to move upwards or downwards in the camera view, which may interfere with the tracking of the object propagation path. So, some common situations had to be excluded from the analysis, such as when the car is stopped at a red light. Therefore, if the car has been stopped for a sufficiently long period, the rUFOV analysis is not performed since it is assumed that there may be driving rules that allow the driver to be passive and not follow other traffic objects. However, when the car starts to move forward, the drivers were instructed to first look for any potential intersecting traffic object.

3.3 Extraction of traffic objects

The obstacle detection algorithm is one of the key components in the real-time UFOV measurement setup. The front camera behind the windscreen recognizes the driving environment and detects the traffic objects that appear in the periphery of the vehicle, either on the left-hand or right-hand side. The objects (i.e., pedestrians and bicycles) are detected with the optical flow algorithm by using information that objects are moving horizontally against a stationary background.

The feature extraction was based on the direction of the object's movement (i.e., objects that move toward the centre from the periphery were detected). This process was performed with an optical flow algorithm, which calculates the vector field, which then estimates the moving regions between the two consequent image frames [10]: image_1 and image_2. This research applied optical flow methods using the specific function available in the Halcon machine vision library of MVTec Software GmbH [11]:

$$(r', c') = (r + u(r, c), c + v(r, c)) \qquad (6)$$

where $u(r, c)$ and $v(r, c)$ denote the row and column coordinates of the optical vector field in location (r, c) The developed algorithm is based on the two parallel tasks: background elimination and moving object detection.

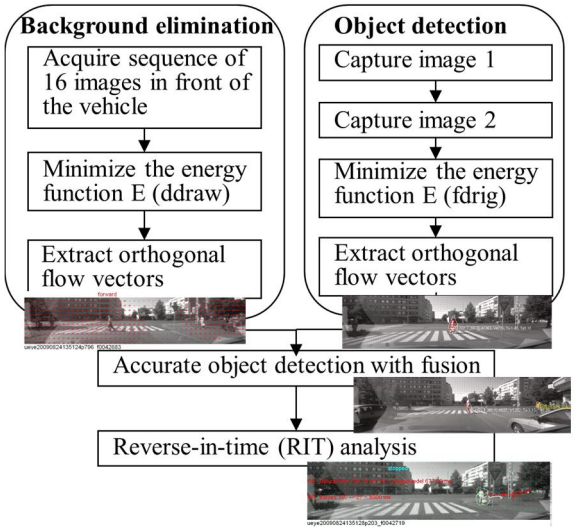

Fig. 6 The optical flow algorithm for object detection in front of the vehicle

3.3.1. Background elimination. Dynamic background modelling with an optical flow method using a spatially smoothed vector field has been adopted to estimate the movement of the background in the perspective direction, caused by the moving camera. For the modelling of background movement, the "draw" algorithm from the Halcon library function was selected [13] which is based on minimising the following energy function:

$$E_{DDRAW} = \int P_{si\_S}\left(f(x+w) - f(x)\right)^2 dr \cdot dc + \alpha \int \left[g(u(x))^T P_{NE} \cdot g(f(x)) g(u(x)) + g(v(x))^T P_{NE} \cdot g(f(x)) g(v(x))\right] dr \cdot dc \quad (7)$$

in the above equation x=(r,c,t) in which (r,c) denotes location and t the time and w=(u, v, 1) is the optical flow vector field to be determined. The term g(f)=(df/dx, df/dy) refers to constancy of the spatial gray value derivate and Psi_S(s2)=sqrt(s2+ε2) is a linear penalization term in which ε =0.001 is a fixed regularization constant. PNE(grad(f(x)) is a normalized projection matrix which is orthogonal to g(f(x)):

$$P_{NE}(g(f(x)) = \frac{1}{g(f(x))^2 + \varepsilon_S^2} \begin{bmatrix} f_c(x)^2 + \varepsilon_S^2 & -f_r(x) f_c(x) \\ -f_r(x) f_c(x) & f_r(x)^2 + \varepsilon_S^2 \end{bmatrix} \quad (8)$$

The algorithm is data-driven and anisotropic, which means that discontinuities in the optical flow vector field are allowed to cross the object edges in the image, and the result is smoothed only across the uniform brightness regions and along the object edges. This approach is an optimal option in the case of background modelling, as many background objects in street scenery include sharp and straight edges, for example buildings, streetlight posts, sign rods, road markings and parked vehicles.

3.3.2. Moving object detection. For detecting the moving traffic objects, for example, pedestrians, cyclists or other vehicles, the 'fdrig' algorithm from the Halcon library function was applied [12]. This algorithm uses the original movement constancy assumption of the gray values, but also adds constancy assumption for the gray value gradients. This latter assumption has the advantage of being more robust with regard to illumination changes that may occur, for example when a pedestrian walks in the shade of trees or buildings. As greater detail is needed to detect moving objects, especially in the case of pedestrians, warping was allowed down to the finest resolution level of the algorithm. The energy function to be minimised in this case is:

$$E_{FGRID} = \int P_{si\_S}\left[\left(f(x+w) - f(x)\right)^2\right] + \gamma\left[g(f(x+w)) + g(f(x))\right]^2 dr \cdot dc + \alpha \int P_{si\_S}\left[\left(g(u(x))\right)^2 + \left(g(v(x))\right)^2\right] dr \cdot dc \quad (9)$$

Fig. 7 shows an example of extraction for moving objects. The example includes two pedestrians approaching from the right hand side and one cyclist from the left hand side. The optical flow algorithm calculates the vector field between each consequent image frame, which shows the approaching direction and strength for each pixel area. Threshold operation with several parameters is applied to the vector field to extract the regions of the objects of interest. The vector fields within the threshold regions are shown with small red arrows in the figure. Each object is followed until it reaches the midpoint of the image.

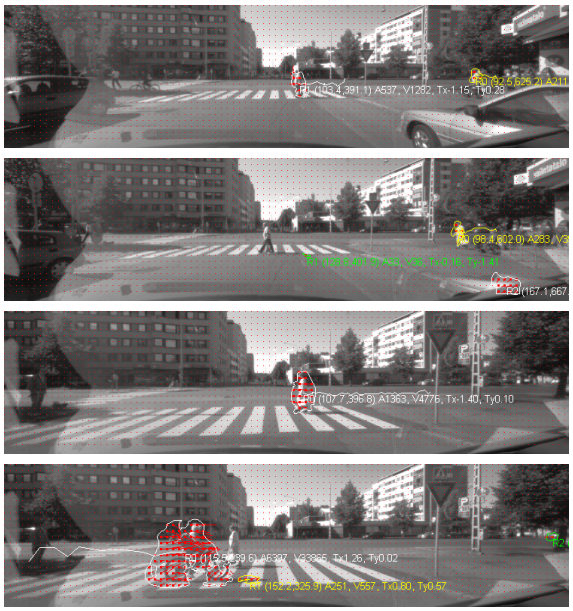

Fig. 7 Extraction of pedestrians and cyclist. The time gap between each selected frame is several seconds, while the actual video frame rate is 10 Hz. The line behind each extracted object shows the propagation path of the center point in the preceding image frames. The parameters displayed for each object show the position, area and movement information, which are to be applied further in the classification

In addition to the optical flow algorithm, the reversed-in-time (RIT) method has been implemented to improve the tracking. The key idea is to analyze the old image frames again and find where the object actually appeared the first time. Of course, this kind of analysis increases latency for the final result, but on the other hand, it improves the sensitivity and reliability for detecting the first occurrences of the objects.

In many cases, the intersecting vehicles or pedestrians are difficult to detect from their first appearance. As the distance with the object is reduced, they become larger in the image plane with better details. When the ego-vehicle approaches the intersection area, the perspective view of the camera causes the slow-moving intersecting pedestrians to appear static or even to move 'backwards' in the image plane. Although this movement differs from the perspective background movement, it makes the extraction still very difficult.

In Fig. 8 and 9, the pedestrian is firstly detected with the optical flow method, which provided the white colored polygon 'tail', showing the movement of the object in the image plane during the previous image

frames. After this detection, we have made shape-matching based tracking for this object from the preceding image frames [14], to find out if it could be recognized even earlier than the white colored polygon shows.

The red-colored polygon shows the result of the RIT-analysis, which performed quite optimally in this example. We can also state that this time the pedestrian did also appear for the first time in the peripheral region of the camera, and we may go back with the driver monitoring data as well and check whether they paid attention to the pedestrian (Time A).

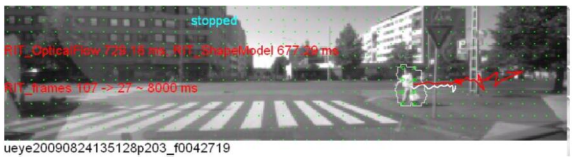

Fig. 8 Result for reversed-in-time (RIT)
This is shown with by the red coloured polygon in to the right side of the detected pedestrian.

Fig. 9 Creation of pedestrian shape model bank,
The image region for shape modeling is first set by the optical flow method.

3.4. UFOV detection in vehicle test

Fig. 10 shows an example of analysis of the driver's attention to peripheral objects. The driver's central vision sector is shown horizontally in each road camera frame with red boxes. To more clearly illustrate the analysis of the driver's viewing angle, the boxes for all five driver camera frames are shown vertically above each other. The middle driver camera frame is closest in time to the road camera frame. The point at which the driver gazes directly at the new object is shown by the vertical red box in the middle driver camera image (Note that the actual road camera frame rate was 10 fps, although Fig. 10 shows only one selected image every half second to illustrate the method.).

Five corresponding frames of the driver camera are shown at the right-hand side of each road camera frame. Together, each group of driver and road camera images covers a one-second time period, and the middle frame from the driver camera corresponds to the timing of the road camera frame. The total time for all five driver camera frames is also shown in the bottom label (labeled "eye-time").

The car was moving slowly in front of a non-priority intersection when a bicycle arrives from the right. The bicycle could be seen in the first road camera frame, but, the optical flow method found it from the second frame, and showed the traced propagation path of the bicycle as a dotted green line in the frame. The white "o" marks in the last frame showed the driver's gaze direction toward the bicycle in the past frames. In the second road camera frame with the middle frame of the driver camera, it was judged that the moving regions of the object and the viewing regions of the object were intersecting with the intersection judgment function according to the equation (1) since the measured coordinate of the bicycle was located between column pixel (u) of 355 and 414, and then, his viewing angle of the central vision (β0 shown in Fig. 3) was 60 ° (Tb) based on the output relates to the measured gaze direction/vector data (at eye-time 513 second). The appearance time of bicycle (Ta) would be estimated approximately at eye-time 511 seconds. Thus, the reaction time (Sc) was 30 (60 ° /2 second).

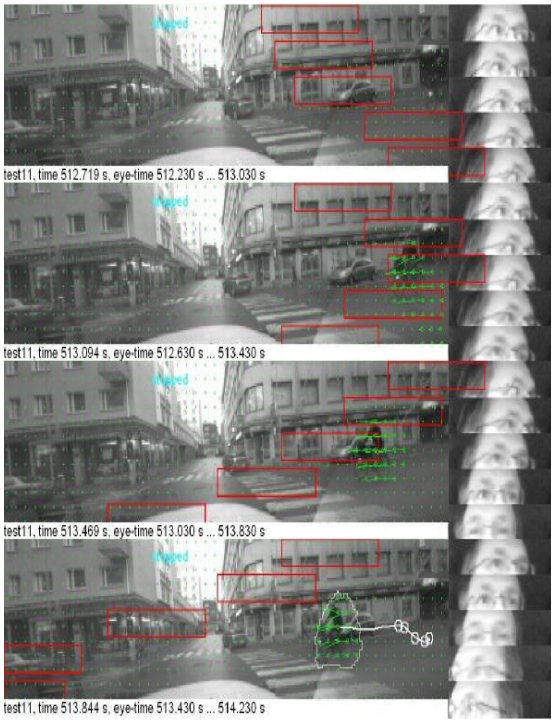

Fig. 10 Example of UFOV analysis

Data for five drivers in Tampere city centre in Finland was collected over approximately 1 hour of driving each. All drivers were male between the ages of 25 and 45. All had normal physiological vision conditions. By running the rUFOV analysis, a total of 123 peripheral traffic objects were identified for the five test subjects. By manual checking of the videos, it was found that 47% of the found objects were cars, 42% pedestrians and 11% bicycles.

Most of these traffic situations occurred when approaching an intersection or pedestrian crossing. A large number of situations with intersecting traffic were not included in this selection, because the driver had

already stopped for a red traffic light. Naturally, there were also many peripheral traffic objects that did not approach the intersection area of the car, and thus were not included in the final analysis. After analyzing the driver monitoring videos, a total of 23 test cases were considered as not-detected events due to the lack of reliable readings of the driver's viewing angle. In most of these cases, the driver's face was obscured by his hand while turning the steering wheel, which indicates that the results might be improved with better placement of the driver monitoring camera. Based on this number of discarded events, the reliability reading of the rUFOV driver monitoring analysis on this test set was 81.1%, where 100 cases succeeded out of a total number of 123 (TABLE 1).

TABLE 1
DETECTION RESULTS

Subject	Detected	Not Detected	Reliability
1	31	5	86.1
2	19	3	86.4
3	17	8	68
4	19	4	82.6
5	14	3	82.4
total	100	23	81.1

Fig. 11 shows another example where Subject 1 did not look (oversight in Fig. 2) at the new object twice from 31 detected test results. In this example, the pedestrian arrives from the left-hand side. Fig. 11 shows the final result with the propagation path with white colour on the image plane, and no incidents were found where the driver would have been looking to the right. However, in this case Subject 1 was already slowing down, because of the pedestrians who were already crossing the street in the middle of the image. To come to a confident conclusion regarding when the driver decided to slow down, it may not be necessary to actively search for any new intersecting objects.

Fig. 11 Example with no glance at the pedestrian (Subject 1)

From the results, it was concluded that this method was suitable for detecting a driver's UFOV while driving. Subsequently, the driving simulation test with the stereo camera based tracking system was introduced to measure the driver's gaze angle precisely.

4. Driving Simulation Test

4.1. Test conditions

4.1.1. Driving simulator (DS). To verify the ability of the proposed method to measure the driver's attention capability in a vehicle test, a stereo-camera based tracking system was used (the faceLAB system created by Seeing Machines) with a 60 Hz frame rate and an information processing system on a driving simulator.

In order to reproduce the rUFOV method under complex traffic scenarios, a test was conducted using the driving simulator shown in Fig. 12. This includes eight near-miss crash scenarios classified with a potential risk level from A (most difficult driving) to C (least difficult driving), depending on how fast the driver can respond to the near-miss crash scenario (TABLE 2)..

The DS was equipped with left and right wing

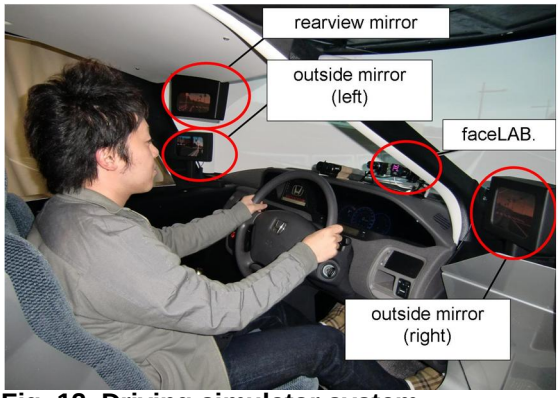

Fig. 12 Driving simulator system

mirrors and a rear-view mirror in the same way as in a vehicle test. The faceLAB camera was fitted at the top of the dashboard to analyze the driver's gaze information. A projector was installed on the ceiling of the DS to project the driving course onto a screen.

TABLE 2
TRAFFIC SCENARIOS AND POTENTIAL RISK LEVEL

Scenario No.	Traffic Scenario	Risk Level
1	Blue sedan merges (interrupts) into the driver's lane from the right	B
2	Truck merges from the left and turns right	B
3	Bicycle suddenly appears from behind a car and crosses the road from the left	A
4	White sedan merges into the driver's lane from the right	B
5	Yellow taxi crosses the intersection from the right	C
6	Truck crosses the intersection from the right	C
7	Child suddenly appears from behind a fence and crosses the intersection from the left	A
8	Silver wagon suddenly appears from behind a fence and crosses the intersection from the left	A

Subjects were instructed to drive this course after an announcement.

4.1.2. Vision angle measurement. As shown in Fig. 13, the driver's gaze and head direction were output as vertical rotation "pitch angle" components (up = positive) and a lateral rotation "yaw angle" component (rotation to left = positive).

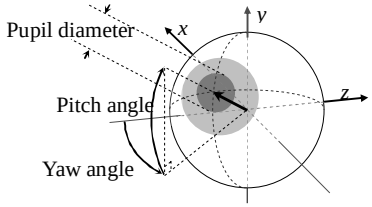

Fig. 13 Pitch and yaw angle

Other information obtained included data from the faceLAB system (head position, head orientation angle, head position tracking quality, eye position, and gaze direction), heart rate (at repose and during driving), driving time, as well as answers from a questionnaire. The questionnaire was given to the subjects just after completing each driving test to obtain a subjective appraisal of the degree of haste and impatience on five levels from 1 (lowest) to 5 (highest).

An increase in mental load was reported to adversely affect the scope of vision range (i.e., to make it more narrow) and to cause the driver's gaze direction to concentrate more on the vehicle's direction of movement [17] [18]. Thus, it was attempted to measure the UFOV under changes in psychological state (normal and hasty driving runs) to verify the effectiveness of the rUFOV method.

The same driving course (route, appearance of objects, traffic signals, and the like) was used for all the tests. To compare the normal driving run with the hasty driving run, the second measurement results for both cases were selected after each test had been completed twice. To realize the hasty driving situation, the subjects were directed to drive faster than the normal driving run, and the safety actions were left to the driver. Due to the specifications of the DS, in the event of an accident such as a crash with another vehicle along the course, the driving simulation stopped while the system recovered and restarted the course from a nearby position.

4.1.3. Heart rate measurement An electrocardiogram (ECG) waveform was measured by the monitor lead method, involving a standard limb lead (II) and three chest electrodes. The instrument used was a Polymate AP1000 (Digitex Lab. Co., Ltd). Ripple noise was removed from the obtained waveform using 4th order Butterworth bandpass filters. Sampling was performed at a rate of 60 Hz with a 5-second time window.

4.2. Driving time, heart rate, and questionnaire results.

Table 3 shows the measurement results for average heart rate and driving time, and the answers to the questionnaire survey for subject A (20 year-old student who drives very frequently), subject B (57 year-old professor who drives very frequently), subject C (33 year-old office worker who drives twice a week), and subject D (42 year-old office manager who drives frequently).

TABLE 3
Measurement Results of Heart Rate, Driving Time, and Questionnaire Survey

Profile	Measured Items	Normal Driving	Haste Driving
Subject A	Heart rate (Frequency/Minite)	84.2	95.3
Male (20 years)	Driving time (m: s: ms)	3:56:03	2:21:53
Test:2009/12/14	Questionaire (1:lowest, 5:highest)	1	5
Subject B	Heart rate (Frequency/Minite)	73.1	81.3
Male (57 years)	Driving time (m: s: ms)	3:55:89	3:04:34
Test:2009/12/21	Questionaire (1:lowest, 5:highest)	1	5
Subject C	Heart rate (Frequency/Minite)	80.41	81.15
Male (33 years)	Driving time (m: s: ms)	3:11:63	2:40:49
Test:2010/5/28	Questionaire (1:lowest, 5:highest)	1	5
Subject D	Heart rate (Frequency/Minite)	84.75	82.18
Male (42 years)	Driving time (m: s: ms)	3:21:30	2:44:64
Test:2010/5/28	Questionaire (1:lowest, 5:highest)	1	5

It was decided to start the hasty driving run after verifying that the heart rate had decreased to its original level before the normal driving run. However, as the heart rate settled down within five minutes, the rest interval was set at five minutes.

All the subjects had a higher heart rate during the hasty driving run than during the normal driving run except D (but this subject rushed showing in his driving time from 3:21 to 2:44. The shorter time for the hasty driving scenario caused the test subjects to feel rushed. Therefore, all subjects answered in the questionnaire that they felt impatience during the hasty driving run (score: 5). Thus, it can be concluded that these conditions generated feelings of haste in terms of both physiological information and subjective evaluation.

4.3. UFOV measurements results

The time at which objects appeared in the driver's peripheral region and the time at which the driver looked at objects within their central vision were extracted from the yaw angle data. This was confirmed manually to verify whether an object was inside the range of vision (within 13 degrees).

The measurement results for the UFOV of subject B are shown in Table 4 for the eight near-miss crash scenarios and Fig. 14 for Scenario No.3. Table 4 shows that the reaction time in the hasty driving run is faster than for the normal driving run for almost all the scenarios, which seems to be due to the difference in driving speeds. Thus, there is a tendency in many cases

of hasty driving for the gaze to turn to objects that are closer to the driver than in normal driving. However, the hasty driving result for scenario No. 3 shows a different result. In this scenario, B's vision range (UFOV) seems to become narrower in the hasty run. In fact, subject B was not intentionally turning his gaze to the bicycle when the bicycle suddenly turned around in his gaze. As a result, the bicycle seemed to appear directly in front of the vehicle in the intersection, resulting in a collision. Subject B attempted emergency braking, but did not react fast enough to stop. In addition, with regard to scenarios 5 and 6, subject B did not turn his gaze at all since he judged the traffic scenes with turning objects not to pose a potential risk. Thus, it may be concluded that, in a hasty state, a driver may neglect to prepare for turning hazards. In these cases, the driver concentrates their gaze more on the central view and less on the peripheral view (caused a reduction in UFOV) (refer to [19] for more cases).

TABLE 4
Measurement Results of UFOV (Subject B)

Sean No.	Risky Level	Normal Driving		Hasty Driving	
		Reaction Time (Sec)	Eccentricity (Degree)	Reaction Time (Sec)	Eccentricity (Degree)
1	B	4.35	24.06	2.95	23.82
2	B	1.40	17.90	0.40	13.64
3	A	1.95	21.74	2.00	13.65
4	B	3.30	27.98	0.00	2.70
5	C	4.60	2.84	No glance	
6	C	0.20	3.02	No glance	
7	A	1.55	12.84	1.30	4.77
8	A	0.95	4.58	0.95	5.32

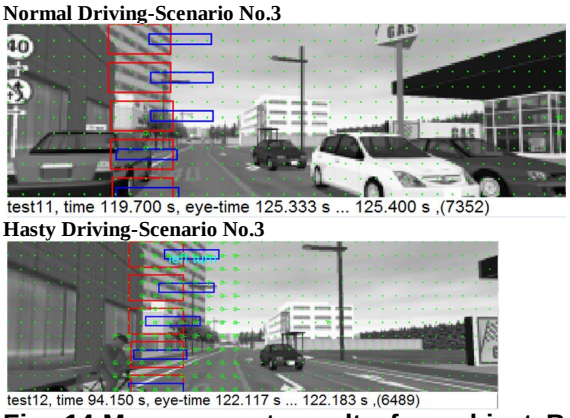

Fig. 14 Measurement results for subject B
The traced propagation path of the object was shown by a green line in each frame. The gaze area of 13° in the red box and the face direction in the blue box are measured from the yaw angle

Table 5 shows the measurement results of the changes in reaction speed according to the equation (4) for the test subjects. The reaction speeds decreased in almost all cases. This means that the size of the UFOV decreases as the driver's mental workload increases for different types of potential risk levels. Furthermore, subject B's reaction speeds are slower in all cases than those of the younger subjects, except in the combination of hasty driving with a potential risk level of B (probably because the low potential risk level is a good match for subject B's skill level). This tendency can be said to be age-related because the slowest driver after subject B was subject D (age: 42). These age differences stand out, particularly in the combination of normal driving and potential risk level B for subject B (7.73 compared to the average of 14.39). Even though subject B was the slowest in the combination of hasty driving with potential risk level A (5.58 compared to the average of 9.93), he had an accident in scenario 3. For older drivers, both the reaction speed of the UFOV and the potential risk level of the traffic scenario in hasty driving must be considered to avoid an accident.

TABLE 5
Reaction speed (degree/sec) change by driving type and risk level

Subject	Risky Level B			Risky Level A		
	Normal Driving	Hasty Driving	Change H/N	Normal Driving	Hasty Driving	Change H/N
A	17.84	7.79	0.44	13.49	10.92	0.81
B	7.73	11.99	1.55	8.80	5.58	0.63
C	13.63	8.16	0.60	25.08	11.99	0.48
D	10.94	5.66	0.52	13.12	8.94	0.68
Average	14.39	6.73	0.47	13.31	9.93	0.75

5. Conclusion

An real-time method for measuring a driver's UFOV (rUFOV) has been developed. In this method, the original laboratory method using a PC display [5] has been expanded to monitor the driver in ordinary traffic during much longer periods. The measurement system includes one video camera for extracting peripheral traffic objects and one for measuring the driver's viewing angle. The real traffic tests indicated that the system technically works with a performance level of 81% and it was measured its reaction time.

By incorporating the rUFOV method into a driving simulation environment, it was possible to conduct safer tests for drivers under reduced visual conditions, such as changes in the driver's mental status (hasty driving), introduced more accurate control parameters into simulation software for more potentially risky driving scenarios, and measured the driver's visual acuity in the central vision based on collected test data.

The accuracy of the automatic image processing was then confirmed and favorable results were obtained for its effectiveness at measuring the driver's UFOV. The rUFOV method can be adopted with real-time driver support or immediate alarm systems, and to the collection of statistical data to identify the visual condition of the driver.

The rUFOV measurement data for each peripheral object can be compared with the results obtained from current UFOV measurement. From this comparison, it is possible to calculate the percentage reduction in UFOV values from past standardized data and the statistical

reliability of the measurement period. The final result can be classified to obtain potential risk statements in different categories to be displayed for the driver, or to be applied further to the driver support system of the car.

6. Further issues

It is necessary to test a large group of elderly drivers with a high variation in visual ability. The simulator environment may also enable a more direct comparison between the original laboratory UFOV [2] measurement method and the rUFOV method to reveal the relationship between a reduction in the UFOV and increased accident potential risk [3].

The results for reduced UFOV may provide supportive information about the driver's vision for driver support system alarms and car control functions. Applications in which such information might be useful may enable automatic HMI adaptation according to the driver's ability, increase the reaction time of the driver when the peripheral view is limited to ensure that approaching vulnerable road users are identified, and provide a positive feeling for the driver when the peripheral view is good, motivating them to pay more attention to roadside events.

7. References

[1] Sims R., McGwin G., Allman R., Ball K., Owsley C.: Exploratory Study of Incident Vehicle Crashes Among Older Drivers, Journal of Gerontology, Medical Science, 2000, Vol. 55A, No. 1, M22-M27

[2] Ball K., Owsley C., Sloane M.E., Roenker D.L., and Bruni, J.R.: Visual Attention Problems as a Predictor of Vehicle Crashes among Older Drivers. Investigative Ophthalmology & Visual Science, 1993, 34, No. 11, 3110-3123

[3] National Police Agency in Japan, "Road Traffic Accidents and Fatalities in 2008, National Police Agency in Japan, February 26, 2009

[4] Owsley C: Visual Processing Impairment and Risk of Motor Vehicle Crash Among Older Adults, JAMA, 1998

[5] EARPA Position Paper 2010. A Vision for Integrated Road Transport Research. European Automotive Research Partners Association."

[6] UFOV User's Guide, Version 6.0.9, Visual Awareness, Inc. 1991, 1996 and 2002. Available at: http://crag.uab.edu/VAI/PDF%20Pubs/UFOV_Manual_V6.0.6.pdf

[7] Summala H., Nieminen T., and Punto M.: Drivers Learn To Rely On Peripheral Vision When Monitoring In-Car Devices. The Journal of the Human Factors and Ergonomics Society, Volume 38, Number 3, September 1996

[8] Open CV computer vision library Available at: http://www.codeproject.com/KB/cpp/TrackEye.aspx

[9] Kutila, M., Jokela, M., Markkula, G. & Rué, M., R. 2007. Driver Distraction Detection with a Camera Vision System. Proceedings of the IEEE International Conference on Image Processing (ICIP 2007). 16-19 Sep. 2007. U.S.A., Texas, San Antonio. Vol. VI, pp. 201-204.

[10] Horn B., and Schunck B.: Determining optical flow. Artif. Intell., vol. 17, pp. 185-203, 1981

[11] HALCON software, version 9.0. MVTec Software GmbH, Munich, Germany, http://www.mvtec.com/halcon/

[12] Brox T., Bruhn A., Papenberg N., and Weickert J.: High accuracy optic flow estimation based on a theory for warping. In T. Pajdla and J. Matas, editors, Computer Vision - ECCV 2004, volume 3024 of Lecture Notes in Computer Science, pages 25-36. Springer, Berlin, 2004

[13] Nagel H.-H., and Enkelmann W.: An investigation of smoothness constraints for the estimation of displacement vector fields from image sequences. IEEE Transactions on Pattern Analysis and Machine Intelligence, 8(5):565-593, September 1986

[14] Solution Guide II-B: Shape-Based Matching. Edition 5, December 2008 (Halcon 9.0), 52 pages, MVTec Software GmbH , München, Germany. Available at http://www.mvtec.com/halcon/download/documentation/

[15] CARE - European Road Accident Database. Available in [http://ec.europa.eu/transport/roadsafety/road_safety_observatory/care_en.htm]. cited on 18 June 2009.

[16] PReVENT-INTERSAFE consortium. 2005. Requirements for intersection safety applications. 2005. Deliverable D40.4

[17] Clay O., Wadley V., Edwards J., Roth D., Roenker D., Ball K.: Cumulative Meta-analysis of the Relationship Between Useful Field of View and Driving Performance in Older Adults: Current and Future Implications, Optometry and Vision Science, Vol.82, No.8, August 2005

[18] Owsley C., Ball K., McGwin G., Sloane M., Roenker D., White M., and Overley T.: Visual Processing Impairment and Risk of Motor Vehicle Crash Among Older Adults: JAMA, Vol 279, No.14, April 8, 1998

[19] Danno, M., Masahiro, M., Kortelainen, J. M. & Kutila, M. Detection of a driver's visual attention using the real-time UFOV method. Proceedings of the 2010 13th International IEEE Conference on Intelligent Transportation Systems (ITSC). Funchal, Madeira Island, Portugal. 19-22 Sep 2010. p. 770-776. 2010

Mikio Danno received his Masters degree in Economics from Bombay University in 1979. Currently he works for Toyota InfoTechnology Center in the advanced technology research area..

Dr Matti Kutila received his Doctoral degree in 2006 and has been working for VTT since 1998. His main research topics are automotive environment perception and driver state monitoring.

Juha M. Kortelainen received his M.S. degree in 1990. He joined the VTT Technical Research Centre of Finland in 2004. His expert knowledge is sensor technology, multivariance signal analysis and machine vision.